HAL open science

Retrospective 70 y-spatial analysis of repeated vine mortality patterns using ancient aerial time series, Pléiades images and multi-source spatial and field data

Emmanuelle Vaudour, L. Leclercq, Jean-Marc Gilliot, B. Chaignon

To cite this version:

Emmanuelle Vaudour, L. Leclercq, Jean-Marc Gilliot, B. Chaignon. Retrospective 70 y-spatial analysis of repeated vine mortality patterns using ancient aerial time series, Pléiades images and multi-source spatial and field data. International Journal of Applied Earth Observation and Geoinformation, 2017, 58, pp.234-248. 10.1016/j.jag.2017.02.015 . hal-01606921

HAL Id: hal-01606921

https://hal.science/hal-01606921v1

Submitted on 27 May 2020

HAL is a multi-disciplinary open access archive for the deposit and dissemination of scientific research documents, whether they are published or not. The documents may come from teaching and research institutions in France or abroad, or from public or private research centers.

L'archive ouverte pluridisciplinaire **HAL**, est destinée au dépôt et à la diffusion de documents scientifiques de niveau recherche, publiés ou non, émanant des établissements d'enseignement et de recherche français ou étrangers, des laboratoires publics ou privés.

Distributed under a Creative Commons Attribution - ShareAlike 4.0 International License

International Journal of Applied Earth Observation and Geoinformation 58 (2017) 234–248

Contents lists available at ScienceDirect

International Journal of Applied Earth Observation and Geoinformation

journal homepage: www.elsevier.com/locate/jag

Retrospective 70 y-spatial analysis of repeated vine mortality patterns using ancient aerial time series, Pléiades images and multi-source spatial and field data

E. Vaudour[a,*], L. Leclercq[a,b], J.M. Gilliot[a], B. Chaignon[b]

[a] UMR ECOSYS, AgroParisTech, INRA, Université Paris-Saclay, 78850, Thiverval-Grignon, France
[b] Domaine des Chauvets, 26110 Vinsobres, France

ARTICLE INFO

Article history:
Received 22 June 2016
Received in revised form 28 January 2017
Accepted 14 February 2017

Keywords:
Digital zoning
Vine mortality
Terroir
Time series
Cross-variogram
EM38
Pléiades
Farm scale
Stock unearthing

ABSTRACT

For any wine estate, there is a need to demarcate homogeneous within-vineyard zones ('terroirs') so as to manage grape production, which depends on vine biological condition. Until now, the studies performing digital zoning of terroirs have relied on recent spatial data and scant attention has been paid to ancient geoinformation likely to retrace past biological condition of vines and especially occurrence of vine mortality. Is vine mortality characterized by recurrent and specific patterns and if so, are these patterns related to terroir units and/or past landuse? This study aimed at performing a historical and spatial tracing of vine mortality patterns using a long time-series of aerial survey images (1947–2010), in combination with recent data: soil apparent electrical conductivity EM38 measurements, very high resolution Pléiades satellite images, and a detailed field survey. Within a 6 ha-estate in the Southern Rhone Valley, landuse and planting history were retraced and the map of missing vines frequency was constructed from the whole time series including a 2015-Pléiades panchromatic band. Within-field terroir units were obtained from a support vector machine classifier computed on the spectral bands and NDVI of Pléiades images, EM38 data and morphometric data.

Repeated spatial patterns of missing vines were highlighted throughout several plantings, uprootings, and vine replacements, and appeared to match some within-field terroir units, being explained by their specific soil characteristics, vine/soil management choices and the past landuse of the 1940s. Missing vines frequency was spatially correlated with topsoil $CaCO_3$ content, and negatively correlated with topsoil iron, clay, total N, organic C contents and NDVI. A retrospective spatio-temporal assessment of terroir therefore brings a renewed focus on some key parameters for maintaining a sustainable grape production.

© 2017 The Author(s). Published by Elsevier B.V. This is an open access article under the CC BY license (http://creativecommons.org/licenses/by/4.0/).

1. Introduction

For any wine estate, or wine region, there is a need for a detailed spatial assessment of areas with homogeneous environmental features that are likely to confer typical wine qualities. Such areas, also named terroir units, are identified through collective memory and conveyed from generation to generation within a territory marked by social context and cultural technical choices (Vaudour, 2002, 2003). Their shaping often inherits a long heuristic process, likely hundreds of years, eventually marked by discontinuities due to war, wine market opportunities and the spread of plagues (Dion, 1990; Unwin, 1991). The differentiation and mapping of regions of grape and wine quality require comprehensive spatial modelling of climatic, soil and agronomical properties, including their changes through time (Vaudour, 2002; Deloire et al., 2005; Costantini et al., 2012; Tomasi et al., 2013). The construction of spatial models for demarcating terroir units and predicting their viticultural and wine response is undergoing a methodological revolution as new technologies and analytical methods enable the capturing of detailed spatial and temporal variability of grapevines according to functional properties in the soil (Vaudour et al., 2015a). The spatial data that may be collected for such zoning may consider seasonal interannual vineyard variability changes through a time series of satellite images (Lanjeri et al., 2004) or integrate

* Corresponding author.
E-mail address: Emmanuelle.Vaudour@agroparistech.fr (E. Vaudour).

http://dx.doi.org/10.1016/j.jag.2017.02.015
0303-2434/© 2017 The Author(s). Published by Elsevier B.V. This is an open access article under the CC BY license (http://creativecommons.org/licenses/by/4.0/).

seasonal changes (Vaudour et al., 2010); however, until now such assessment has been made with recent data that were currently available at the time of the mapping, regardless of the fact that cumulated past choices may reflect vine behaviour and soil quality according to vineyard management. Some recent approaches carried out for the purpose of within-field terroir units or management zones delineation combined a set of field observations with several recent spatial layers, mainly morphometric data being derivatives of a digital elevation model, and/or vegetation index derived from remotely sensed data and/or proxy-sensed soil apparent electrical conductivity (ECa) (Pedroso et al., 2010; Rossi et al., 2003; Priori et al., 2013). In addition to demarcate homogeneous within-vineyard zones, there is a need, in cases where the winegrower starts up its activities, to retrace the behaviour of these zones in the past, so as to consolidate the diagnosis of vine biological condition, and determine further adoption of new soil and vineyard management practices that are likely to favour a long-term preservation of quality production together with soil ecosystem functions. Moreover, as terroir is by definition a spatial entity constructed and recognized over a long duration, terroir assessment should be addressed considering a large span of years. Yet, to date, scant attention has been paid to ancient geoinformation about the past biological condition of vines and the occurrence of vine mortality in particular, that is long term terroir response. At the farm scale, is vine mortality characterized by recurrent and specific patterns and if so, are these spatio-temporal patterns related to terroir units and their present-day vine biological condition and soil properties? Are they, else, related to past landuse patterns? Is vine mortality spatially structured and spatially correlated with perennial soil properties or is it spatially correlated with dynamic soil properties under the influence of past soil management? Soil management and, in overall, viticultural techniques, reparcelation and land-leveling by heavy machinery, that have been developed by intensive viticultural systems since the 1970s, have caused soil degradation, particularly in Mediterranean environments (Lagacherie, 2005; Costantini and Lorenzetti, 2013). Soil degradation was hypothetized as the driving factor for the vine decline, and hence mortality, that has been reported in Languedoc as soon as the 1990s (Legros et al., 1998).

In this study, over the currently existing vineyard of a farm undergoing new ownership and needing to recapture time pass, we aimed at: (i) performing such historical and spatial tracing of vine mortality patterns, over the span of 70 y using a long term series of remotely-sensed images; (ii) digitally mapping within-field terroir units using multiple spatial layers; (iii) then testing the mapped mortality patterns against terroir units and their current soil and vine condition parameters. The study was original in constructing a map of missing vine frequency from the photograph time series along with the panchromatic Pléiades band of 2015, while digital within-field terroir units were obtained from a supervised classifier (support vector machine) computed on the spectral bands and NDVI of Pléiades images, EM38 data and morphometric data. The validation of the within-field terroir units relied on their degree of matching with groups of topsoil properties.

Vine condition was assessed through field observations aiming at characterizing vine vigour, and the NDVI computed from the summer Pléiades image. Because the studied vineyard displayed distinctive erosion features, and because erosion was demonstrated to cause nutrient depletion (Ramos and Martínez-Casasnovas, 2006), and therefore damage vine biological condition, a further issue raised by this study deals with the rapid assessment of soil erosion intensity and its influence on mortality patterns. In addition to the commonly observed trunk or bunch field measurements, the vine-stock unearthing-burying simple method proposed by Brenot et al. (2008), abbreviated as 'stock unearthing measurement' (SUM), was used as a means to characterize occurrence and intensity of soil loss. The SUM approach was first proposed by Brenot et al. (2008) in Burgundy, and consists in measuring the distance between scion-graft union and soil surface, representing a benchmark of soil surface displacement since the year of plantation. Provided planting age and modalities be known (Brenot et al., 2008; Casalí et al., 2009; Paroissien et al., 2010; Quiquerez et al., 2014), the SUM approach efficiently quantifies erosion and deposition rates, particularly for Mediterranean vineyards (Casalí et al., 2009; Paroissien et al., 2010).

2. Materials and methods

2.1. Study area

The study zone is a 6 ha-farm of the Vinsobres appellation (Côtes-du-Rhône, Southern Rhone Valley, France), the "Domaine des Chauvets" estate, planted with rainfed Grenache noir, Syrah, Carignan, Mourvèdre and Roussanne (44°19′06″–44°19′44″ N; 5°0′46″–5°1′22″ E, WGS, 1984) (Fig. 1). Vine spacing is 2.5 m between rows and 1 m between vines within a row. The training mode is either the provençal gobelet or the Cordon de Royat. According to a previous study carried out at the regional level (Vaudour et al., 1998; Vaudour, 2003), soil landscapes and potential terroir units that may be found at the farm level are characterized by a diversity of soils including Red Mediterranean soils (chromic luvisols), colluvic calcisols, arenosols, fluvisols, and regosols (World Reference Base, 2014), which develop from top to slope then bottom of a Neogene molassic and conglomeratic plateau. The general approach conducted is presented in Fig. 2. It relies on the gathering of multi-source information on soils and vines (soil survey, geophysical prospection, recently acquired imagery), and the restitution of the 70 y-history of the farm through both survey to former winegrowers and the processing of ancient aerial photographs time-series. The latter enables to derive past landuse and the long-term frequency of missing vines.

2.2. Field observations

2.2.1. Soils and soil surface condition

A field survey comprising 14 soil pits was carried out in January 2015 and soil profiles were described according to the STIPA-2000 standard system in France (Falipou and Legros, 2002). Locations of soil pits relied on the local adaptation of the set of rules of soil landscape organization previously defined for the surrounding region (Vaudour et al., 1998; Vaudour, 2003). A series of 98 additional soil surface samples was collected over the farm plots following a stratified random sampling scheme according to observed variations in soil surface conditions.

All soil profile horizons and soil surface samples had physicochemical analyses for conventional parameters: particle size fractions (NF X31-107), soil organic carbon (SOC) content, calcium carbonate content (NF ISO 10693), iron content after Mehra and Jackson (1960) extraction, total N (NF ISO 13878), pH in water (NF ISO 10390). The SOC content of these soil samples was determined by dry combustion at 900 °C according to the French norm NF ISO 10694. This technique provides the total C content, so that for calcareous samples, a correction was applied from the determination of total carbonate (NF ISO 10693). The SOC content of calcareous samples was determined by subtracting carbon content from carbonates to total carbon content.

For the horizon having the highest vine root density at each soil pit, analyses of exchangeable cations (Ca, Mg, Na, K, Fe, Mn, Al) by cobaltihexammine chloride dosing (NF ISO 23470), of EDTA-extractible ions (Cu, Fe, Mn, Zn) (NF X 31-120 and NF ISO 22036), of exchangeable P by the Olsen method (NF ISO 11263), of active

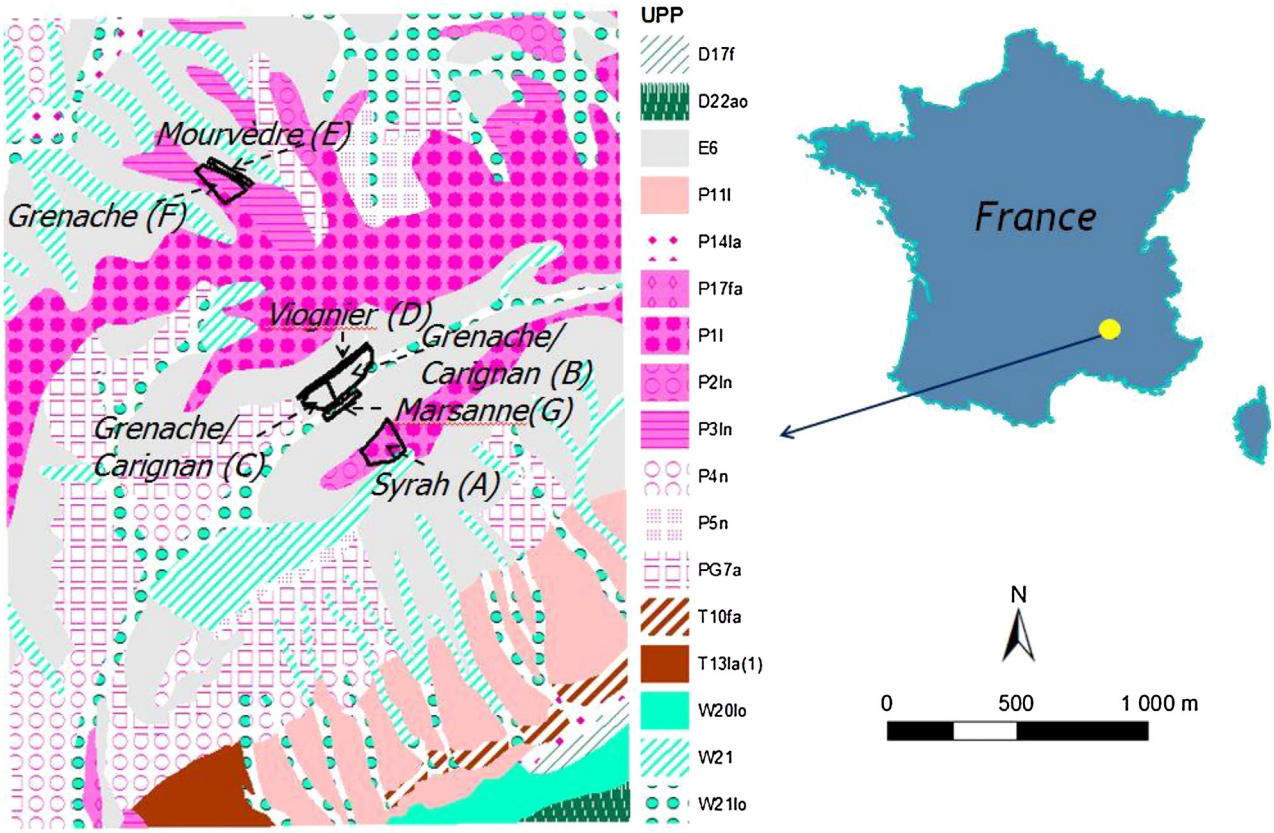

Fig. 1. General soil map derived from the regional soil landscape map (Vaudour et al., 1998; Vaudour, 2003), location of vine varieties within farm plots (in capital letters). D17f, D22ao: stagnic calcaric cambisols, fluvisols; E6, colluvic leptosols; P11l, P14la, colluvic pachic cambisols; P17fa, P1l, P2ln, P3ln, haplic/eutric skeletic petrocalcic cambisols (chromic); P4n, P5n, PG7a, colluvic, skeletic, anthrosols (escalic), petrocalcic calcisols; T10fa, T13la(1), chromic skeletic luvisols, cambisols; W20lo, W21, W21lo, skeletic fluvisols, colluvic regosols.

Table 1
Main characteristics of the studied scenes.

Scene	satellite	Resolution (m) Multispectral/ panchromatic modes	Time of acquisition (U.T GMT)	Viewing zenith angle (°)	Sun azimuth (°)	Sun elevation (°)	Spectral bands
18 May 2014	Pléiades 1B	2.0/0.5	10:41:44	3.5	150.39	62.86	B. (b0), G. (b1), R. (b2), NIR. (b3)
28 July 2015	Pléiades 1A	2.0/0.5	10:38:20	6.4	144.84	61.07	B. (b0), G. (b1), R. (b2), NIR. (b3)

Legend: B. blue; G. green; R. red; NIR. near infrared.

lime (NF X 31-106), of copper content by the $CaCl_2$ dosing (INRA method), were carried out.

Soil surface condition was also qualitatively described in the close vicinity of each pit and in the inter-row for each soil surface sample: presence/absence of sparse vegetation, the presence of coarse fragments, crop debris or organic manure, soil crust.

2.2.2. Individual vines

At each of the 112 soil sampling locations in January then in May 2015, an individual vine was selected and described for biological parameters including stock-unearthing height, vine trunk circumference, basal diameter of the bunch peduncle (January) and vigour, presence of diseases or nutrient deficiencies (May). Because of our studied area similarities in pedoclimatic conditions and viticultural system, the consistency of the plantation of vine-stocks, and a mean initial elevation of the graft union of 2.5 cm, as verified in Languedoc by Paroissien et al. (2010), were assumed for the studied farm.

Concerning both vine circumference and basal diameter of the bunch peduncle, they were observed because of their known relationship to vine key ecophysiological parameters along with their easiness of measurement in the field. According to Pedroso et al. (2010) vine trunk circumference is correlated to the normalized difference vegetation index (NDVI). The NDVI itself relates to the leaf area index (LAI: the ratio of leaf surface area to ground area), fractional cover, biomass, shaded area (e.g. Hall et al., 2003; Johnson, 2003; Dobrowski et al., 2008) and grape quality (Fiorillo et al., 2012). As for basal diameter of the bunch peduncle, Castelan-Estrada et al. (2002) demonstrated that it best predicted the dry mass of a grape for Vitis Vinifera L. 'Merlot' vines.

2.3. Spatial data

2.3.1. Recently acquired spatial data

2.3.1.1. Pléiades satellite images. Two Pléiades satellite images with 2.8 m (multispectral mode) or 0.7 m (panchromatic mode) reso-

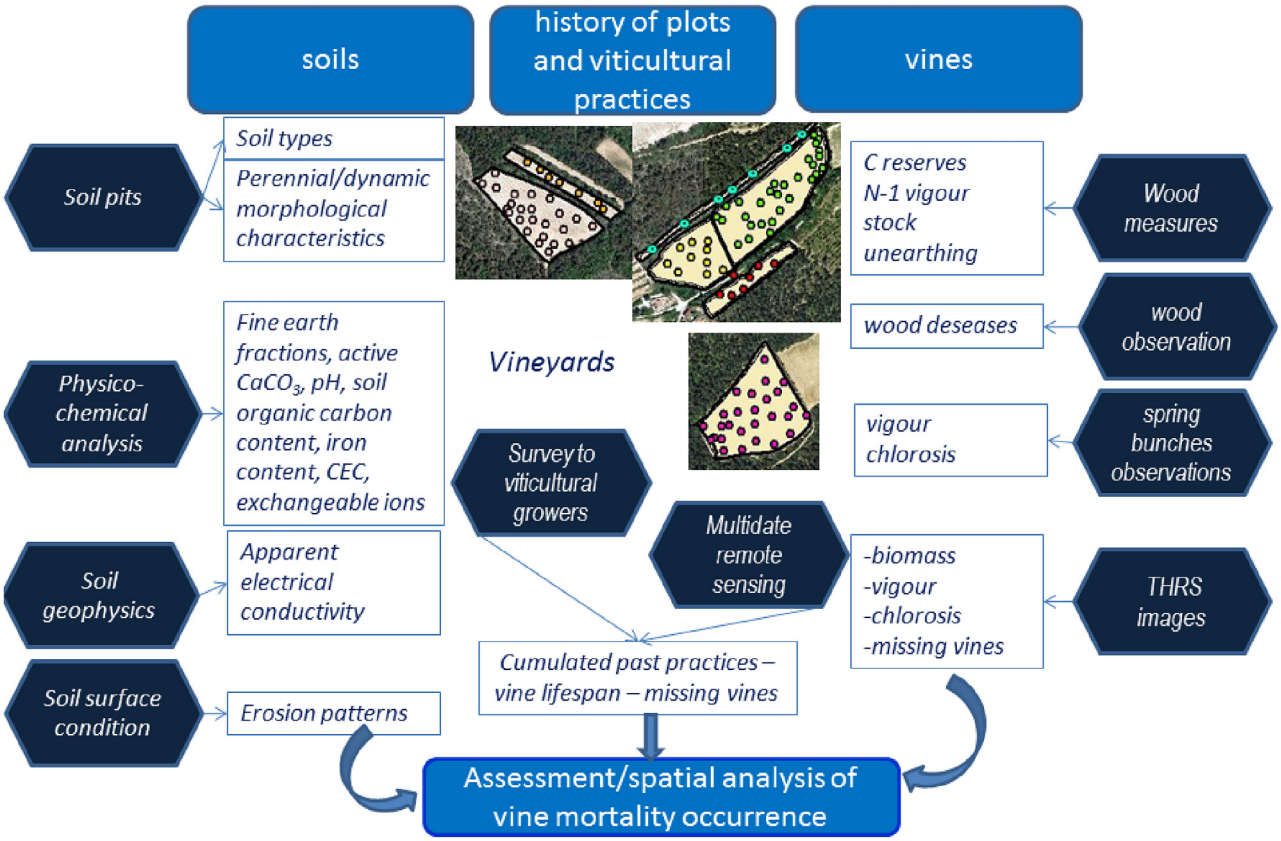

Fig. 2. General flowchart of the approach.

lution were acquired under clear sky over the study area on 18 May 2014 and 28 July 2015. The Pléiades sensor has 4 spectral bands (b0, 0.43–0.55 μm; b1, 0.50–0.62 μm; b2, 0.59–0.71 μm; b3, 0.74–0.94 μm). Both Pléiades images were delivered as 'Ortho' product (Astrium GeoInformation Services, 2012) with resampling at 2 m and 0.5 m-resolutions in multispectral and panchromatic modes, respectively (Table 1) and a radiometric quantization of 12 bits.

Full scenes were clipped to obtain subscenes of approximately 800 m × 1180 m (Fig. 1) that focused on the study area. We performed atmospheric corrections of the Pléiades images with the ATCOR2 predefined mode for multispectral sensors, flat terrain, constant atmospheric condition, no haze removal and the default calibration file, the accuracy of which ranges between ±2% and 4% reflectance out of backscattering regions (Richter and Schläpfer, 2014; Vaudour et al., 2014b).

2.3.1.2. Proxy-geophysical survey. Electromagnetic induction ECa measurements were made at a total of 532 point locations across the farm plots in January 2015. The EM38 meter (Geonics), having a coil separation of 1 m and operating at a frequency 14.6 kHz, was used in both horizontal dipole and vertical dipole modes, thus providing depth of investigation of 0.75 and 1.5 m, respectively. ECa measurements were performed manually and were randomly sampled through walking along the inter-rows.

For each measured location, the geographical coordinates were recorded with a 50 cm accuracy using a Trimble® Pathfinder POWER DGPS. Maps of ECa were constructed by inverse distance weighting interpolation at a 5 m-resolution.

2.3.1.3. Morphometric data. In order to account for morphometric features in the digital zoning, the digital elevation model (DEM) RGEALTI2.0 elaborated by the French National Institute of Geographic and Forest Information (IGN) at a spatial resolution of 5 m was used and ten derivatives (slope, aspect, shaded relief, profile/plan/cross-sectional/longitudinal convexities, minimum and maximum curvatures, quadratic error of elevation) were calculated within a 3 × 3 window. The topographic modelling module of ENVI5.3® (Harris) was used.

2.3.2. Long term aerial photograph time-series

A time-series of ancient aerial photographs in digital format was downloaded from the Geoportail website of the IGN, and was composed of various emulsions acquired between 1947 and 2001 (Table 2). Each photograph was georeferenced under ArcGIS10.2® using the colour 2010-orthophoto of the IGN as geographical reference for selecting ground control points and either 2nd order polynomial or spline function was used for geometrical correction; output resolutions were comprised between 0.3 and 1.4 m. The visual interpretation of the whole time-series along with a survey to the former winegrowers of the farm enabled to construct the timeline of past landuse and past viticultural practices over the span of 70 y.

2.4. Zoning approaches

In this study, the digital detailed zoning of within-field homogeneous terroir units was carried out using the varied set of recently acquired spatial data. For both past landuse and missing vines frequency, the mapping was performed using selected photographs amongst the long term aerial photograph time-series jointly with the panchromatic Pléiades image of 2015.

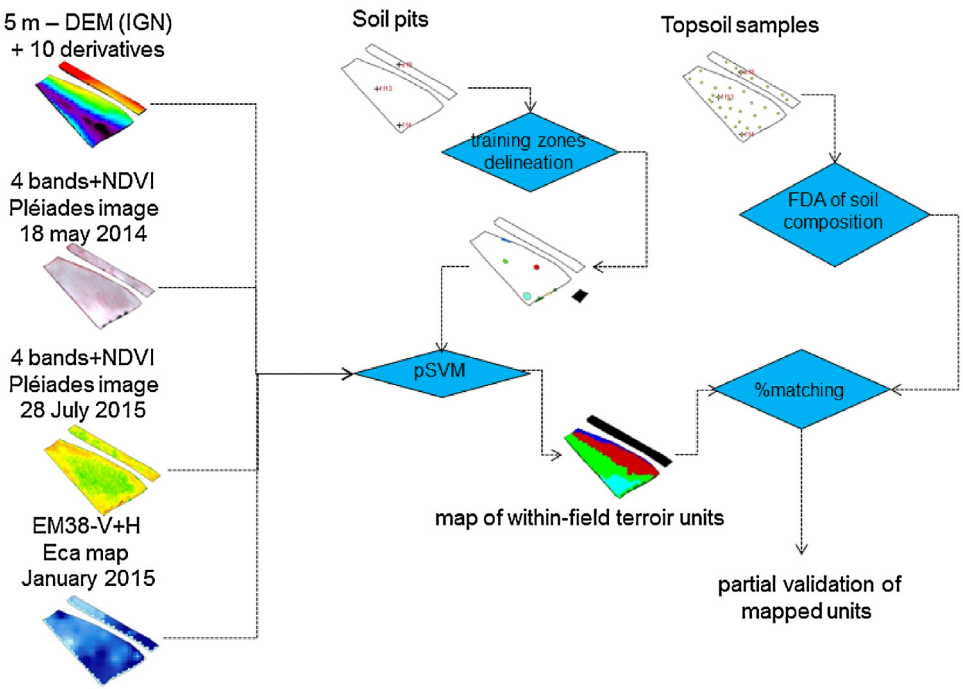

Fig. 3. Flowchart of digital zoning approach to map within-field terroir units using most recent data.

2.4.1. Within-field terroir units

Within-field terroir units, aimed at generalizing soil profiles and vine observations made at each soil pit, were mapped for each of the main fields of the farm: from North to South, F (1.3 ha), BC (2.4 ha), A (1.6 ha). A multilayer image comprising 23 bands (the 4 original bands of each Pléiades image and their NDVI band, elevation and 10 derivatives, horizontal and vertical dipole ECa) was constructed for each of the studied fields (Fig. 3). Training areas were selected in the neighbourhood of each representative soil pit and used to calibrate the support vector machine classifier with polynomial function (pSVM). The reason for this classifier choice is that it is known to outperform other classifiers when addressing landuse/crop mapping (Pal and Mather, 2004; Löw et al., 2013) and particularly when using Pléiades imagery (Vaudour et al., 2015b) using a small training set (Pal and Mather, 2004). Owing to the fact that native resolution is slightly higher than vine inter-row spacing, pixels are mixed pixels ('mixels') composed of vine vegetation, bare soil, shadows, and eventually grass (only in the lower part of the BC field). The overall assumption made when using Pléiades multispectral data is that the bitemporal mixed signal is likely to footprint the characteristics of each within-field terroir unit, jointly with the other spatial data.

Assuming that within-field terroir units should exhibit homogeneous soil composition, the validation of pSVM classification results was performed using the additional topsoil samples. For each field, a factorial discriminant analysis (FDA) was performed on the set of topsoil composition variables (clay, loam, silt and sand contents, total nitrogen, C/N, SOC, total $CaCO_3$ and total iron contents). The percentage of correctly predicted within-field terroir units was retained as a criteria of pSVM validation.

2.4.2. Mapping of past landuse and missing vines frequency

Past landuse was mapped from the visual interpretation of two key aerial photographs: those acquired in 1947 and 1972.

The mapping of missing vine frequency followed the process described in Fig. 4. Key dates were chosen in order to piece the main changes together, using the best resolved photographs and notably the infrared coloured and coloured emulsions, together with the 50 cm-panchromatic image of 28 July 2015. Each greyscale image (or its red band in case of colour or infrared colour) was then segmented through the ENVI-FX® object-image classifier. The 'segment only' feature extraction module with either intensity (most images) or edge algorithm was used and varying scale (35–70) and merge levels (50–99) and texture kernel sizes (5–19) were manually parameterised in order to automatically extract patterns of vine vegetation and 'holes' of missing vines into a shapefile. The 'holes' polygons were then visually selected, carefully verified, eventually reshaped then completed from visual interpretation in order to build a map of missing vines. Each map of missing vines was then converted into raster format then binarised (with value 1 for missing vines areas) and the sum of all binary images resulted into the raster map of missing vines frequency.

Vines rows were visually interpreted and the total length of 2015-missing vines was retrieved from intersecting the 2015-shapefile of missing vines with that of vine rows; hence estimating the current total number and proportion of missing vines.

2.5. Statistical and geostatistical analyses

Considering either the whole dataset or subsets of the 112 sampling locations according to vine varieties or fields, Chi^2 tests were carried out between soil characteristics, past landuse, missing vine frequency and vine characteristics, in order to examine the possible footprint of past landuse, soil, and viticultural practices on missing vine frequency. However, as Chi^2 tests assume the independency of samples, and are no longer valid when observations are spatially structured (Schabenberger and Gotway, 2005), the structures of spatial dependence were also explored through experimental variograms and cross-variograms were built with couples of quantitative variables, in order to evidence their spatial correlations. Calculations were carried out with the statistical software R and packages gstat2.5.1 (Pebesma, 2004, 2014).

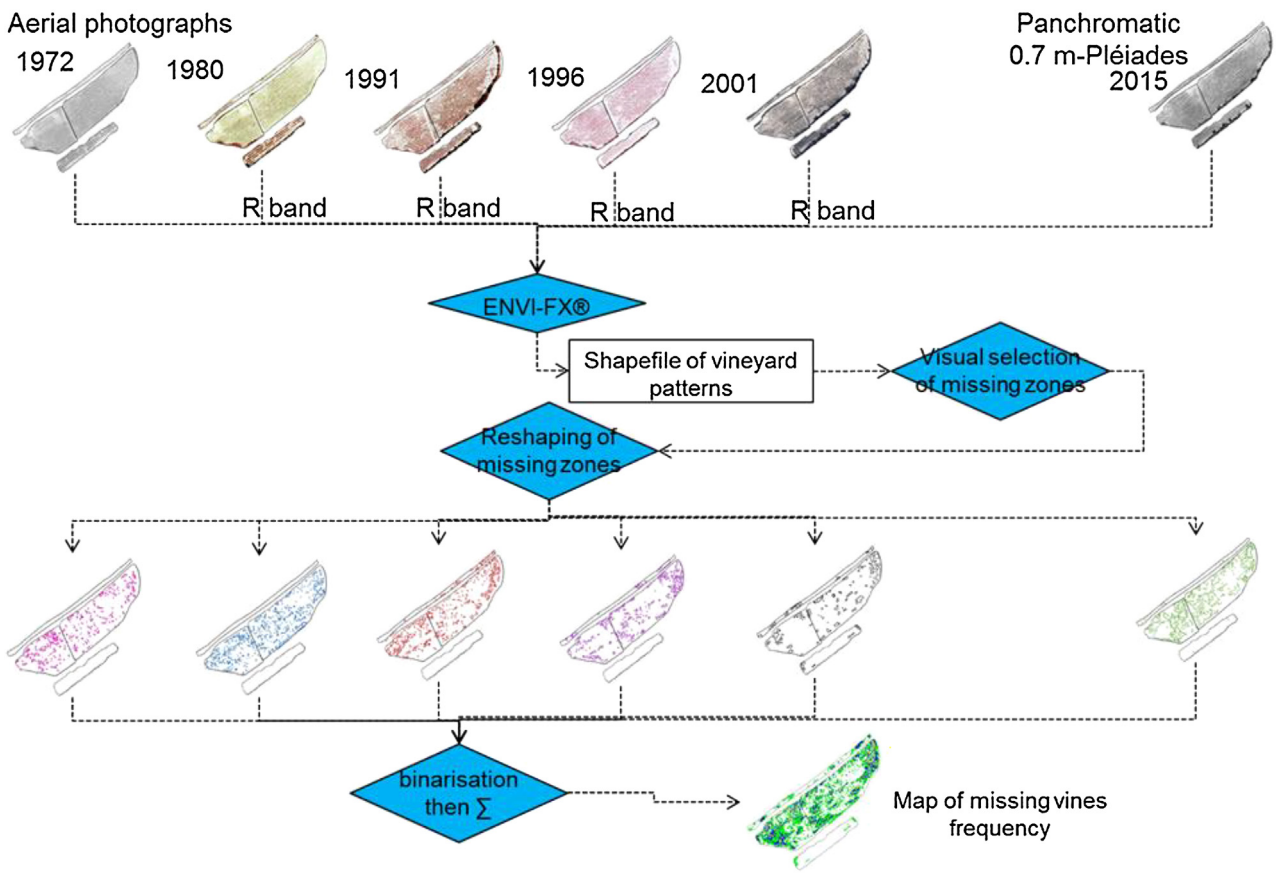

Fig. 4. Flowchart of digital zoning approach to map missing vines frequency using the time series.

3. Results

3.1. Historical timeline for the farm plots

Analysis of the long term aerial photograph time-series revealed a complex history of landuse and viticultural management over 70 y (Fig. 5). According to the survey to former winegrowers, the BC plot was planted with Carignan (grafted on 110R) in 1944, but not on the whole plot area.

This was confirmed through examining the 1947-photograph, which displayed shrub vegetation in its southwestern part, and an orchard in the northeastern part. In 1947, all other plots were occupied by wood, except for plot F which was cropped over 2/3 of its area, presumably with annual crop, as no sign of vine row emerged in the further years, until the clearing of surrounding wood followed by the planting of vine (Grenache grafted on 110R) in 1970. The first vine rows were clearly interpretable in 1976. In the same year, the wood that occupied plot A was cleared and vine was planted with Syrah grafted on SO4. As for plot BC, the northeastern orchard was uprooted in 1955 then the southwestern shrub was cleared in 1965, both followed by the planting of Grenache variety (grafted on 110R). Missing vines appeared in 1972 for plot BC then 1980, for both plots A and BC and further years for plots A, F, BC. For plot BC, patches of Grenache/110R vines were planted in order to fill the 'holes' of missing vines in 1991, 1996 then 2001. Vines in plot F were uprooted in 1998, followed by a new planting of Grenache/110R in 2001, trained in Cordon de Royat. Neither plot A nor plot BC has never been uprooted in its whole area, and the oldest vines there are now 40 and 72 years old respectively, with some former holes of missing vines replaced by younger vines. The survey to former winegrowers indicated the farm was managed with conventional tillage, vineyard rows and inter-rows being weeded chemically. However, there has been no use of chemical fertilizers since 2007 at least, for economic reasons. This resulted in overall weakening of vineyard: yields decreased to less than 30 hl/ha; many missing vines were thus visible in the present-day vineyard. Moreover, nutrients such as K, Mg and P were totally depleted for the horizons having the highest root density (Table 3), which corroborated foliar symptoms of mineral deficiencies in the vineyard. In conjunction with the shortage of chemical fertilizers, applications of herbicides decreased, and grass has been developing in the lowest part of BC plot. Erosion marks were clearly visible for plot BC as soon as the seventies and particularly in the 1978-photograph.

3.2. Within-field terroir units

Fig. 6 shows maps of within-field terroir units obtained from pSVM classifier after smoothing classification results through a median 3×3 filter. Except for FF4 (rendzic calcisol (stagnic)), all other units were characterized by a high proportion of coarse fragments, mostly in the form of limestone pebbles originating from the Miocene conglomeratic alluvial formation. The main characteristics which differed between units were the following: main rooting depth (shallow <50 cm for fields A and F, deeper for field BC); the presence of petrocalcic or calcic horizon; the presence of chromic fersiallitic horizon implying both high clay and iron contents, in addition to high CEC (units AF1 and BF5); the presence of sandy marls as underlying parent material (units FF4 and AF6).

The percentage of correctly assigned soil surface samples to within-field terroir units through the FDA of topsoil sample composition reached 90.5%, 89.2% and 87.0% for plots F, BC and A respectively. This validated the pSVM construction of within-field

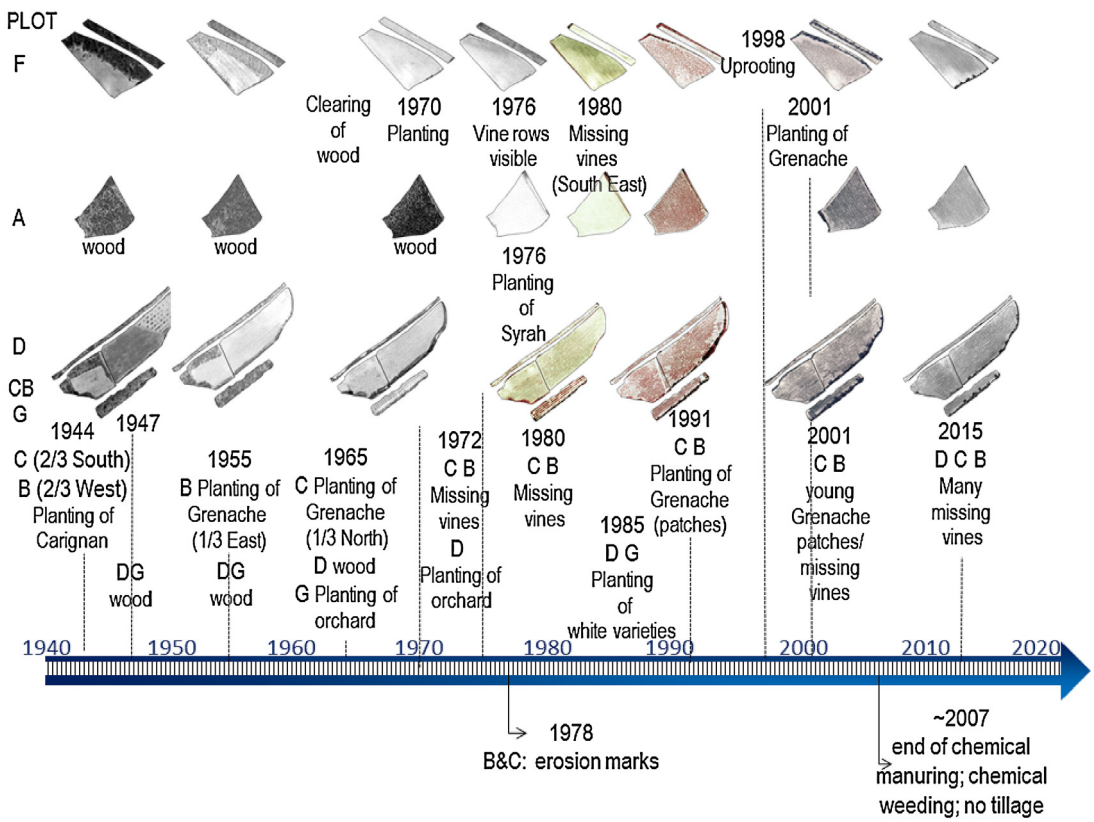

Fig. 5. Historical timeline of landuse and vineyard management.

Table 3
Main characteristics of the studied soils for the horizon having the highest root density within the biggest plots A, B, C and F.

Plot	A	A	A	A	B	B	B	C	F	F	F
Pit	af1	af6	af7	af11	bf3	bf2	bf14	cf9	ff4	ff13	ff5
Texture (FAO)	clay	clay loam	clay	silty clay loam	silt loam	silt loam	silt loam	silt loam	silt loam	silty clay	silty clay
Depth (cm)	10–50	22–45	10–50	12–52	12–42	12–47	20–70	17–57	25–35	12–35	0–25
Root abundance (scale 1–4)	3.5	3.0	4.0	2.0	3.0	3.0	2.0	1.0	2.0	3.0	3.0
Total $CaCO_3$ content ($g.Kg^{-1}$)	90	180	117	277	469	386	400	377	639	264	237
Active lime ($g.Kg^{-1}$)	3.8	4.7	3.9	9.1	11.2	11.2	13.0	13.0	21.8	9.1	7.6
EDTA-extractable iron ($mg.Kg^{-1}$)	18.3	17.4	16.3	14.4	10.3	12.0	12.4	12.0	6.9	13.1	17.5
CEC ($cmol+.Kg^{-1}$)	27.8	26.9	30.4	28.1	13.4	16.0	15.7	17.1	14.3	27.1	29.7
K/CEC (%)	1.0	1.0	1.0	1.0	2.0	2.0	3.0	1.0	1.0	1.0	1.0
Mg/CEC (%)	2.0	2.0	2.0	1.0	3.0	3.0	4.0	2.0	2.0	2.0	5.0
Organic carbon content ($g.Kg^{-1}$)	9.0	11.6	12.6	13.5	6.1	7.9	8.2	7.9	8.2	11.2	12.4
Olsen exchangeable P ($g.Kg^{-1}$)	<0.005	<0.005	<0.005	<0.005	<0.005	0.01	0.01	<0.005	<0.005	0.01	0.01
$CaCl_2$-extractable copper ($\mu g.\ Kg^{-1}$)	45.7	53.7	54.0	41.2	27.7	28.3	42.8	25.1	29.9	48.7	52.2
EDTA-extractable copper ($mg.Kg^{-1}$)	2.05	3.47	4.50	2.59	2.13	2.38	3.80	2.18	1.58	3.89	8.94
EDTA-extractable Zn ($mg.Kg^{-1}$)	0.87	0.84	1.01	0.78	0.55	0.57	0.59	0.73	0.49	1.00	1.75
EDTA-extractable Mn ($mg.Kg^{-1}$)	7.65	7.28	8.37	6.64	3.25	3.67	3.76	3.63	2.85	4.53	7.43

Table 2
The dataset of aerial photographs (IGN).

Emulsion type	Number	Acquisition dates
Panchromatic	19	1947/08/30, 1948/08/15, 1955/03/15, 1956/06/22, 1961/06/17, 1970/05/27, 1972/06/18, 1976/11/17, 1978/08/12, 1979/07/22, 1981/06/15, 1985/06/28, 1988/07/07, 1991/05/25, 1996/06/06, 1998/03/14, 1999/07/01
Infrared –colour	3	1980/06/05, 1991/07/19, 1996/07/31
Colour	3	2001/06/14, 2001/07/12, BD-ortho (April-June 2010)

terroir units from spatial satellite, morphometric and EM38 data as it was consistent with soil surface characteristics.

In term of NDVI quartiles across all farm plots for the Pléiades satellite image of 28 July 2015 (Fig. 7), plots A and F had lower NDVI values than plot BC in overall. This was mainly due to the fact that the lowest part of BC plot had weeds in inter-rows. Within-field units differed by their predominant NDVI quartile class: units FF4, AF7 displayed very low vigour (NDVI < 1st quartile 0.35); units FF3,

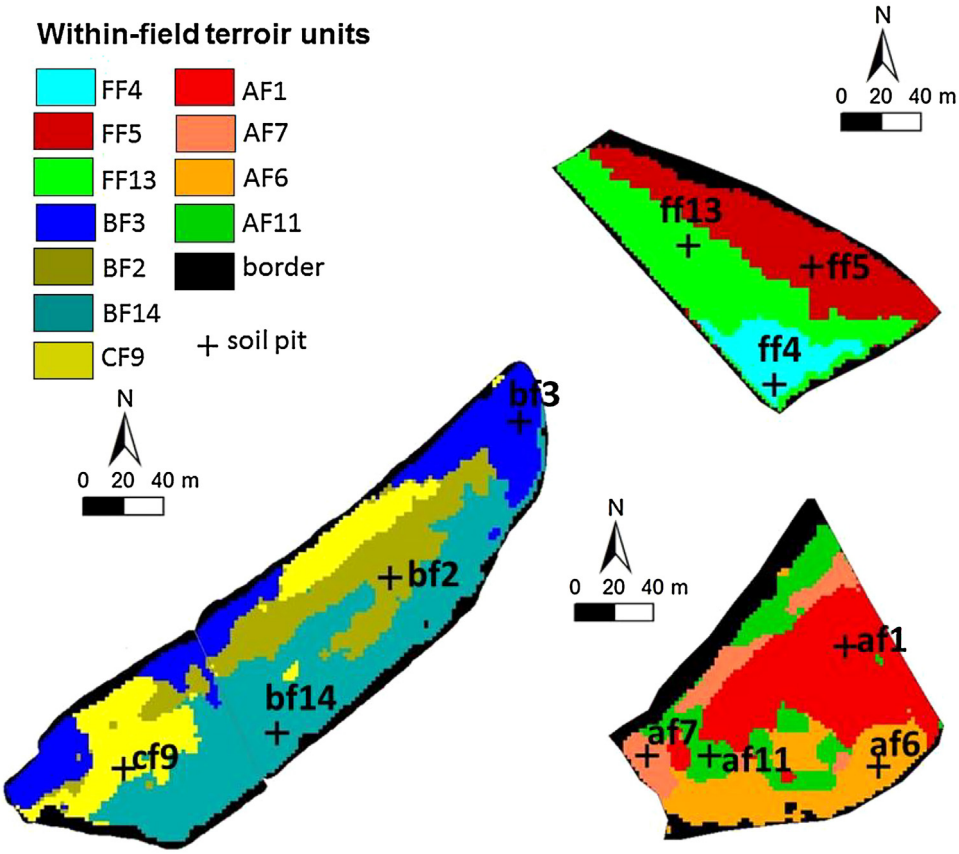

Fig. 6. Maps of within-field terroir units and location of soil pits. FF4, rendzic calcisol (stagnic) over sandy marls; FF5, skeletic petrocalcic cambisol (chromic); FF13, skeletic petrocalcic cambisol; BF3, deep skeletic calcaric fluvisol; BF2, skeletic, colluvic calcaric regosol; BF14, deep skeletic, colluvic calcic regosol; CF9, deep skeletic, colluvic petrocalcic regosol; AF1, skeletic petrocalcic chromic cambisol; AF7, skeletic petrocalcic cambisol (chromic) over sandy marls; AF6, thin skeletic, colluvic petrocalcic cambisol; AF11, skeletic petrocalcic calcaric cambisol.

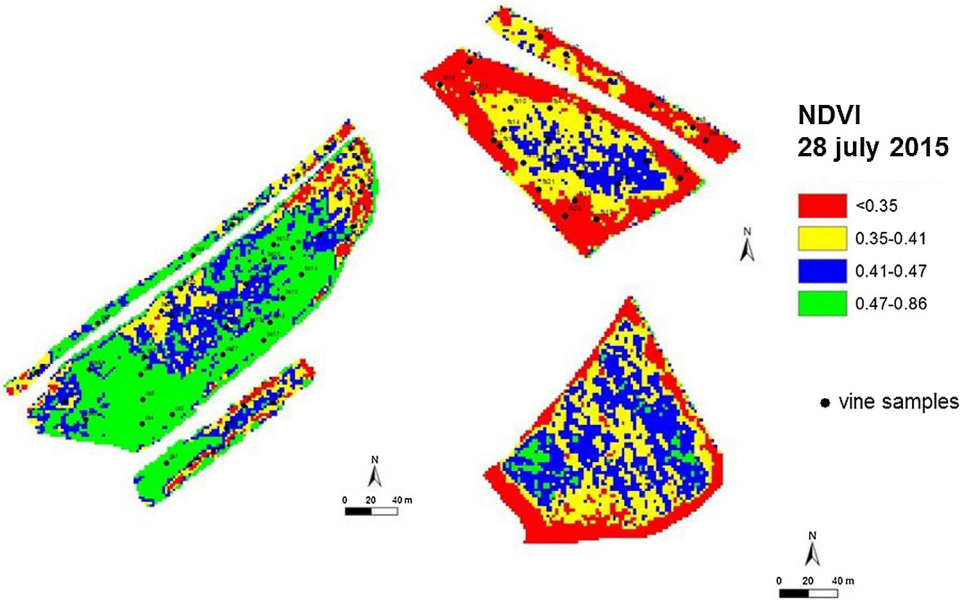

Fig. 7. Map of NDVI quartiles for the Pléiades image of 28 July 2015.

FF5, BF3, AF6 had medium low vigour (NDVI 0.35-0.40); units AF1, AF11 had medium to high vigour (0.41–0.47); units BF2, BF14, CF9 had very high vigour (>3rd quartile 0.47). For units FF4, BF14, CF9, AF1, the predominant quartile class involved more than half of their pixels, while, for the remaining, it was comprised between 1/3 and 1/2.

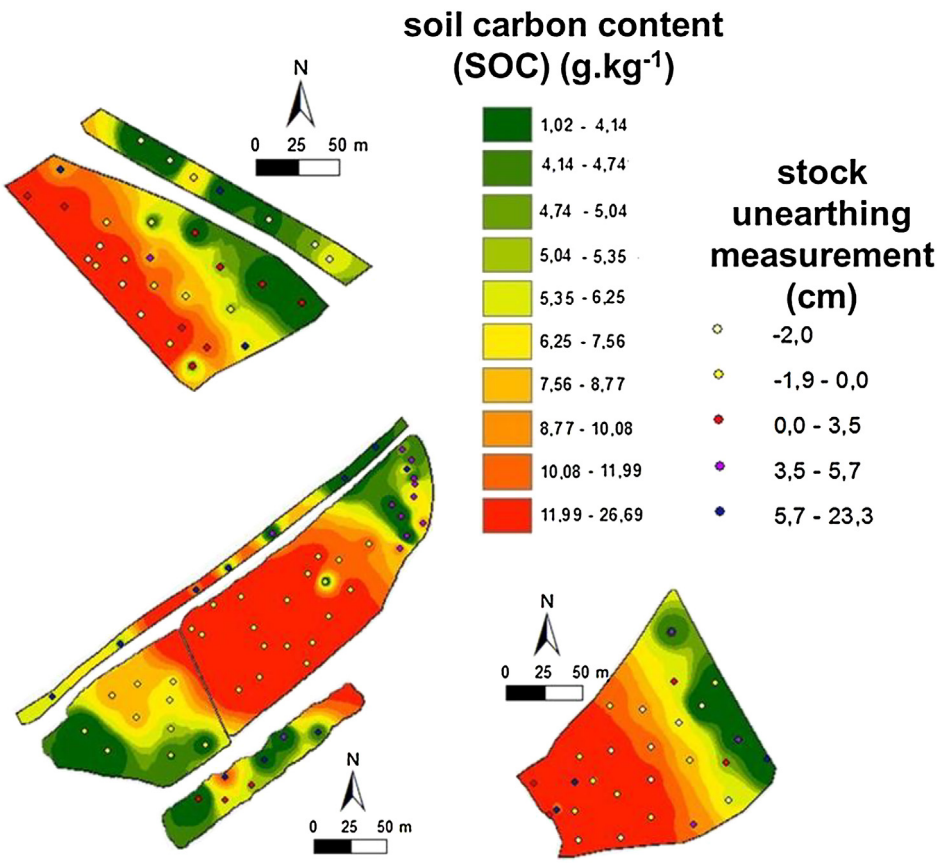

Fig. 8. Maps of topsoil horizon SOC content and point values of stock unearthing height.

Over the whole farm area, SOC contents ranged from 1.0 to 26.7 gKg^{-1} (Fig. 8). Units BF3, FF5 and AF1 exhibited the highest range in SOC contents values and the lowest median values, being 4.9, 5.9 and 7.5 gKg^{-1}, respectively, along with stock unearthing.

3.3. Patterns of vine mortality over time

From 1972–2015, the total area of zones with missing vines increased from 0.18 to 1.01 ha, with a temporary decrease from 1996 to 2001 (0.86–0.68 ha) due to the plantings of patches of Grenache vines in BC plot 'holes' in the early-nineties. For a total of about 17700 initial vine plants, the present-day percentage of missing vines was estimated at 16.9%, which fall in the category of high mortality rate according to a former regional study conducted across the Languedoc viticultural area (Lagacherie et al., 2001). The map of missing vines frequency revealed repeated patterns of higher vine mortality over time (Fig. 9). Such patterns were in adequacy with within-field terroir units, particularly for plots A and BC.

Missing vines were the most frequent for the FF4 and BF3 units, for which they occurred between 3 and 5 years out of 6 observed years. For plot F, shallow root profiles were observed, and in the case of FF4 unit, vine mortality patterns were consistent with low density of observed roots. Whatever within-field terroir unit for plot F, soil profile depth hardly went beyond 90 cm (Fig. 10), owing to a cemented petrocalcic horizon in units FF13 and FF5, and a calcic stagnic horizon for FF4. The weakness of root system development observed for the rendzic calcisol (stagnic) of unit FF4 may be partially explained by concurrent unfavourable characteristics: very high chlorosis index induced by high active lime content (Table 3), medium low CEC and no more nutritive ions consecutively to the shortage of chemical fertilizers, low iron content, low SOC content, in addition to hydromorphic behaviour below 35 cm depth. Unsuited rootstocks may have been chosen for the past plantings, for instance the 110R rootstock variety chosen for the 2001-planting in plot F is not resistant to wet conditions (Galet, 1991a). However the cemented horizon characterizing the two other within-field terroir units implies a limited water available capacity (estimated to about 60 mm for both units FF5 and FF13), which conversely prompts to recommend a rootstock resistant to both drought and chlorosis (that the 110R actually is).

For plot BC, and particularly the BF3 unit, a high stock unearthing height was observed. The higher frequency of vine mortality observed was not evidenced from root profile development, which was dense in the first 50 cm (not shown), but high active lime, medium low CEC and also the shortage of fertilizers nutrients accelerated by soil erosion might play a detrimental role. Owing to the geographical positioning of the BF3 unit at the bottom of a talweg, vine weakness and mortality frequency might be favoured by repeated torrential floodings loaded with pebbles which may collide and damage vine trunks, together with causing erosion.

For plot A, the Syrah/SO4 pair may not be successful for some clones according to Galet (1991a), owing to incompatibility between scion and rootstock. Moreover, SO4 is not resistant enough to drought and has trouble assimilating magnesium.

3.4. Relationships between present-day and past vineyard, and soil

According to Chi^2 tests, the frequency of missing vines was significantly related to past landuse of the 1940s, soil type (in plots BC and F), and in a lesser extent, topsoil SOC content (Table 4).

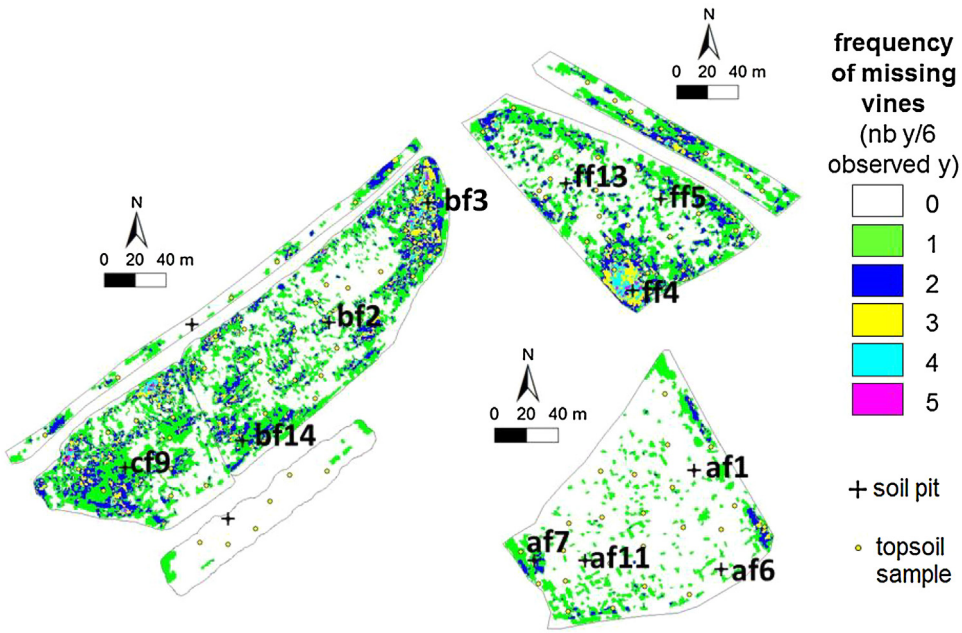

Fig. 9. Map of missing vines frequency.

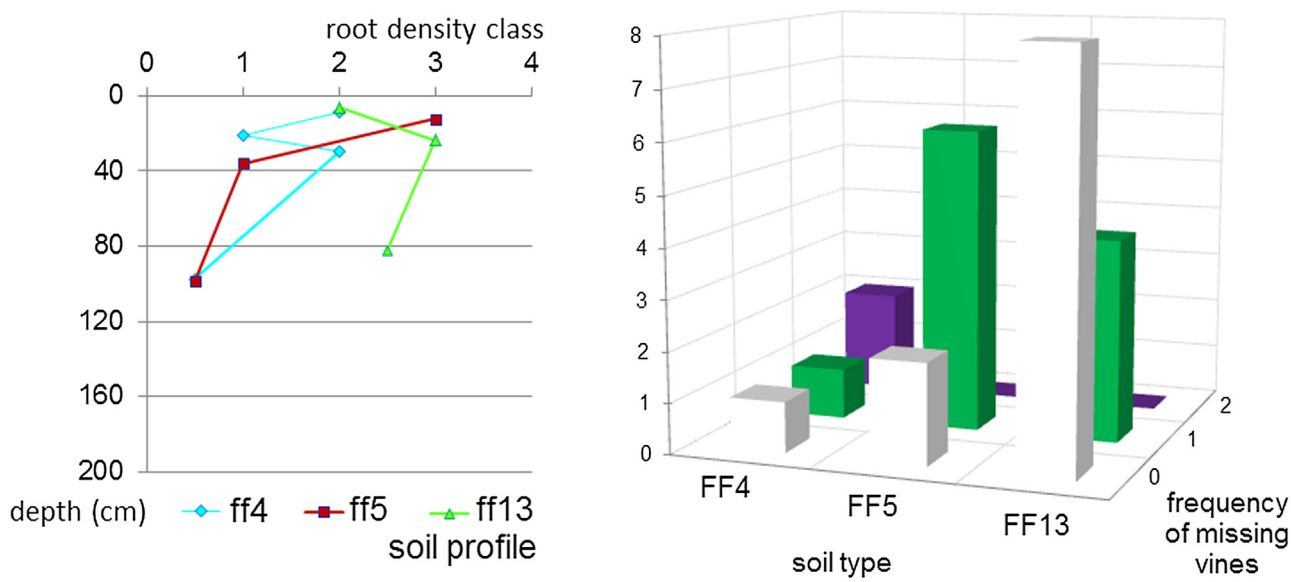

Fig. 10. Root profiles by soil type (left) and 3D[HYPHEN]view of contingency table between soil type (or within-field terroir unit, F plot) and missing vine frequency (right, 24 sample locations). "0", null; "1", 1 or 2 years out of 6 observed years; "2", ≥ 3 years out of 6 observed years. Root density class: 1, very few roots (<8/dm^2); 2, few roots (8-16/dm^2); 3, numerous roots (16-32/dm^2); 4, high density of roots (>32/dm^2).

The 1947-landuse also impacted trunk perimeter, the basal diameter of bunch diameter (*sar*), summer NDVI (Fig. 11). It was also related to *SUM*, which, in turn, was significantly dependent on SOC content. Soil type appeared to relate to past landuse, as some fields were formerly occupied by wood, or by orchard.

The long term frequency of missing vines exhibited no spatial structure when considering the whole dataset (Fig. 12) but was slightly structured and characterized with a 200 m- range for the Grenache variety only (Fig. 13).

It had a spatial negative correlation with the planting age, which is logical considering that the oldest vines were still alive. All other quantitative variables were spatially structured (Figs. 12 and 13), particularly *SUM* and SOC content, *sar*, and topsoil C/N ratio. The cross variograms between *SUM* and the soil parameters showed a spatial correlation with *SUM* only for SOC content (negative), and the calcium carbonate content (slightly positive). The cross variograms between the frequency of missing vines and soil parameters show spatial correlations: negative for iron, clay and SOC content, and positive for calcium carbonate content. For the Grenache variety only, in addition with the negative spatial correlation with planting age, there was a negative spatial correlation with topsoil total nitrogen content, and the summer NDVI (Fig. 13). This emphasised the foreseeable influence of nitrogen on vine vigour.

Table 4
Chi-square statistics between key vine and soil parameters (quartiles classes) or past landuse (observed Chi^2 value, *p-value*, sample size), significance level (*), 0.1; *, 0.05;**, 0.01; ***, 0.005. *SUM*, stock unearthing measurement; *sar*, basal diameter of the bunch peduncle; *nb_manquan*, frequency of missing vines.

Parameter	*nb_manquan*	Trunk perimeter	*sar*	Pléiades NDVI of 28 July 2015 (one variety)	*SUM*	1947-landuse
sar	NS 8.7, *0.19*, 49	* 14.8, *0.022*, 33	–			
Pléiades NDVI of 28 July 2015	NS 7.5, *0.28*, 49	NS 4.1, *0.669*, 33	** 21.6, *0.01*, 49	–		
SUM	NS 10.0, *0.12*, 34	NS 8.3, *0.22*, 33	* 20.4, *0.016*, 34	NS 9.9, *0.36*, 34	–	
1947-landuse	* 17.0, *0.03*, 112	*** 16.8, *0.002*, 33	*** 23.8, *0.005*, 49	** 21.8, *0.01*, 49	** 16.5, *0.01*, 42	–
Topsoil SOC	(*) 11.0, *0.09*, 111	NS 10.1, *0.12*, 33	(*) 14.6, *0.1*, 49	NS 10.8, *0.29*, 49	** 21.1, *0.01*,34	*** 56.5, < *0.0001*, 111
Soil type, plot A	(*) 18.2, *0.052*, 27	NS 7.4, *0.599*, 26	NS 6.5, *0.686*, 26	NS 14.0, *0.121*, 28	NS 11.5, *0.241*, 28	–
Soil type, plots B&C	* 17.7, *0.039*, 40	–	NS 6.8, *0.660*, 25	* 18.5, *0.030*, 25	–	*** 23.0, *0.001*, 40
Soil type, plot F	*** 14.5, *0.006*, 24	NS 3.6, *0.734*, 24	NS 0.6, *0.995*, 24	(*) 11.8, *0.067*, 24	NS 6.3, *0.394*, 24	** 9.1, *0.011*, 24

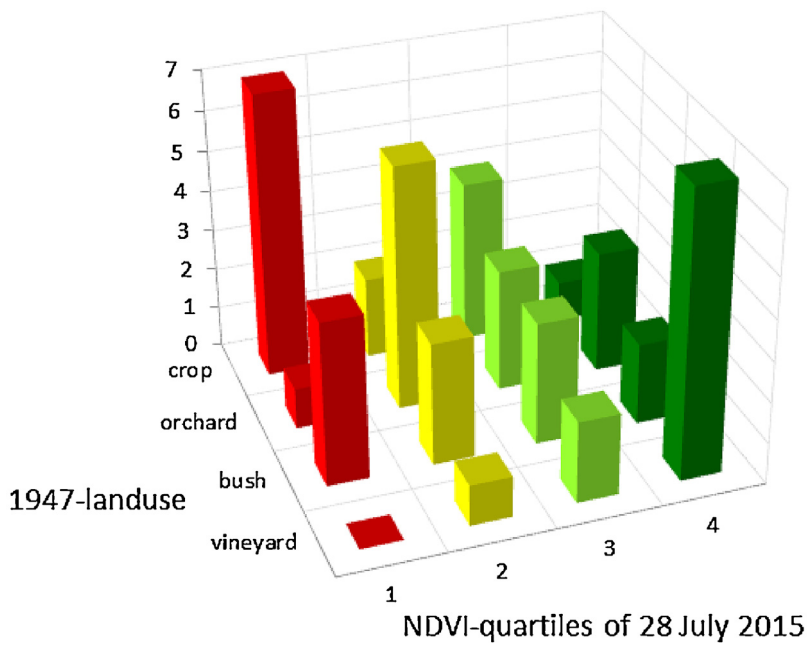

Fig. 11. 3D-view of contigency table between NDVI quartiles of the Pléiades image and 1947-landuse.

4. Discussion

4.1. Original perspective given by the long term spatial-historical approach

The use of the long-term aerial photograph time series enlightened close relationships between soil characteristics and vine response for terroir units at the within-field scale. As a matter of fact, some of these units revealed a higher occurrence of vine mortality. The mapping of the within-field terroir units was guided by previous knowledge on soil landscape and viticultural terroirs in the region (Vaudour et al., 1998; Vaudour, 2003) and by the assumption of the determinant role of soil (in interaction with vintage weather) for vine response, which a number of previous studies evidenced (e.g., Seguin, 1986; Van Leeuwen et al., 2004; Pellegrino et al., 2004; Tardaguila et al., 2011; Costantini et al., 2015; Tomasi et al., 2015). Topoclimatic spatial variability was not studied as such but was indirectly accounted for through morphometric data. Analysis of the historical time-series not only enriched the digital terroir zoning approach compared to that generated only from recently acquired spatial data, but also reinforced it. The zoning approach of within-field terroir units was fully digital and was validated through surface samples. For the mapping of the long term frequency of missing vines, we did not chose a fully automatic approach, owing to the irregular shapes and ages of vines; however the object-image classifier played a facilitating role.

4.2. Accuracy and applicability of the approach

The accurate mapping of both long term frequency of missing vines and current number of missing vines was enabled by very high spatial resolution data with limited positioning error (<1 m). The prediction accuracy of the within-field terroir units obtained from multilayer pSVM classification was higher than 87% according to the set of additional soil sample characteristics. It might be increased collecting proxy-ECa measurements at another season: as a matter of fact, ECa measurements were done under very

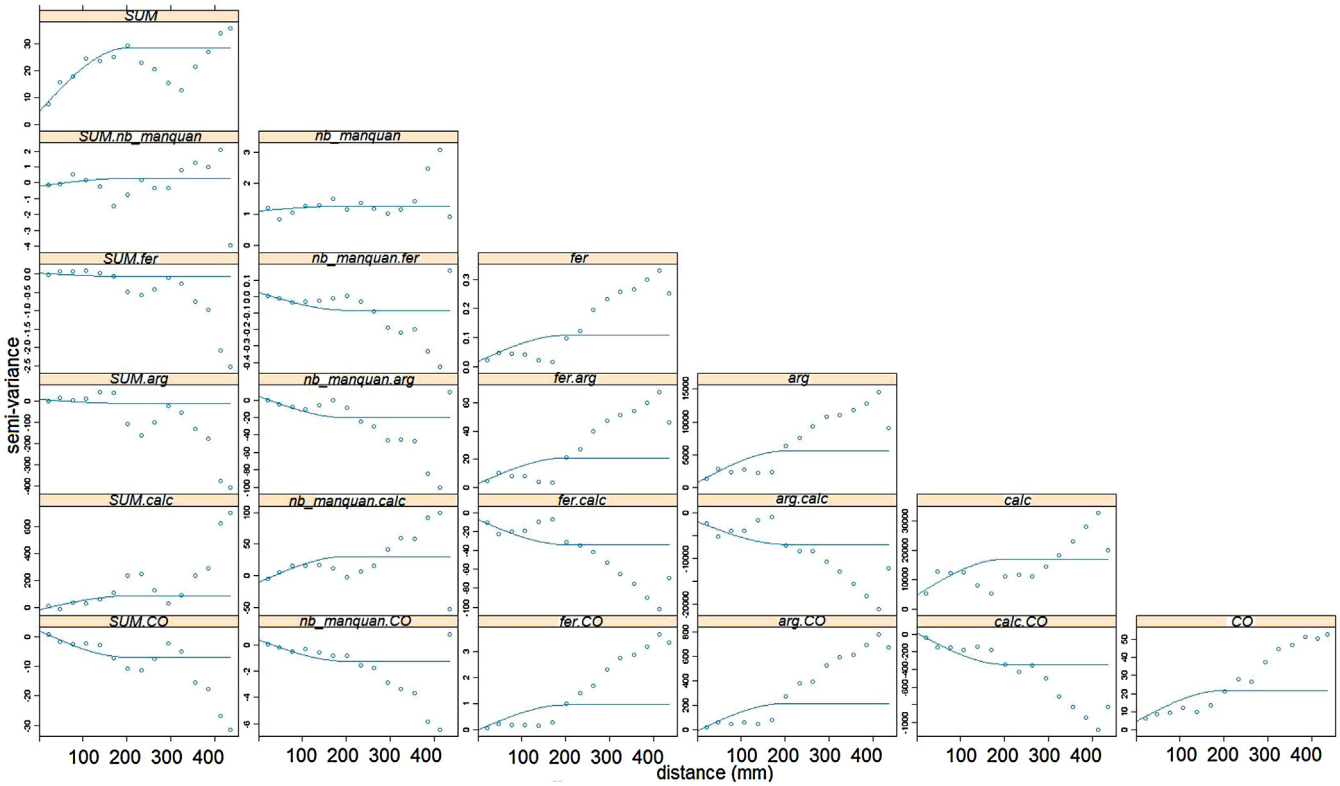

Fig. 12. Cross-variograms between the set of quantitative variables for 111 samples (spherical model, range 200 m). *SUM*, stock unearthing measurement; *nb_manquan*, frequency of missing vines; *fer*, iron content, *arg*, clay content; *calc*, calcium carbonate content; *CO*, SOC content.

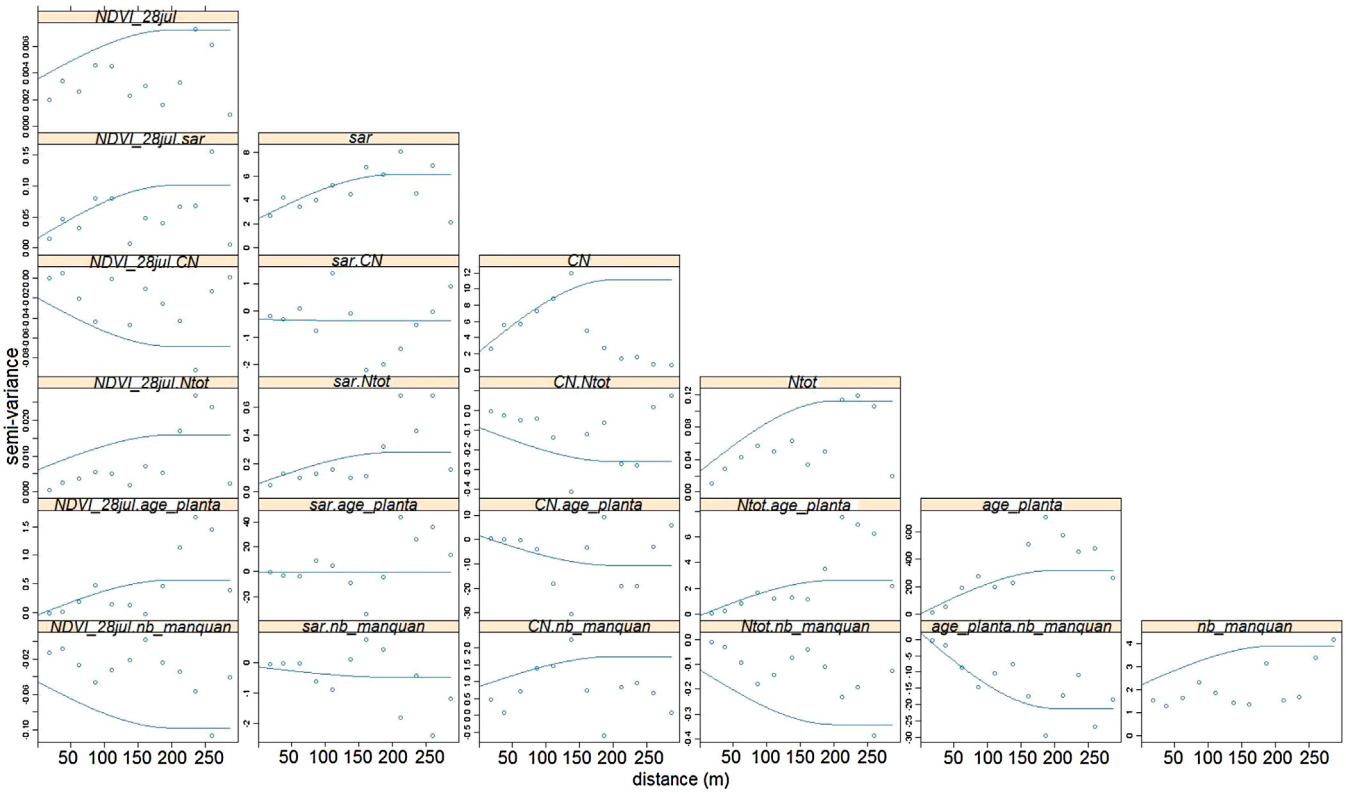

Fig. 13. Cross-variograms between the set of quantitative variables for the Grenache variety (49 samples, spherical model, range 200 m). *sar*, basal diameter of the bunch peduncle; CN, C/N ratio; *Ntot*, total nitrogen content; *age_planta*, planting age; *nb_manquan*, frequency of missing vines.

wet conditions and could be more contrasted in medium moisture conditions.

A full validation of viticultural terroir units would have consisted in considering grape composition at these additional locations, as previously achieved regionally jointly with grape composition time series of 15 y (Vaudour et al., 1998) or 17 y (Vaudour, 2003); however, owing to the diversity in plant material and age, and the fact that terroir response may not be correctly apprehended from one vintage only, this was not carried out.

As regards retracing of vine mortality patterns, the availability of satellite imagery with very high spatial resolution such as Pléiades (70 cm) opens promises for further application of this approach in the years to come. Moreover, in accordance with European directives such as Directive 2007/2/EC of the European Parliament and of the Council of 14 March 2007 establishing an Infrastructure for Spatial Information in the European Community (INSPIRE), that facilitates access and diffusion of spatial information, times series of ancient aerial survey are more and more available in viticultural regions. As they may be available with orthorectification and as mosaics, their use could be extended to larger areas, like viticultural districts. For regularly shaped vineyards, a fully automatic approach could be possible. Additionally, for the component of the approach focused on the retrieval of present-day vine biological condition, the phenology of the present-day vineyard could be assessed using seasonal SENTINEL2 times series as anticipated through SPOT4-Take 5 (Vaudour et al., 2014a).

4.3. Renewed questions about grapevine weakening

The retrieving of missing vine frequency over a long period contributes to renewed questions about the determinism of vine decline. In addition to presumably ill-adapted choices of rootstock varieties for new plantings, the individually replaced vines within former “holes” of missing vines appeared more vulnerable to weakening, hence to mortality: as a matter of fact, they may have encountered difficulties in establishing their root system, all the more than this material was neither resistant to chlorosis and/or drought or to seasonal hydromorphic conditions. Nevertheless, factors other than rootstock choice may have been influential. When searching the Web of Science with the terms “grapevine decline”, or “grapevine weakening”, the studies mentioning it mainly refered to grape diseases, especially wood diseases (Larignon et al., 2009; Bruez et al., 2014), but also viruses (Palomares-Rius et al., 2012; Beuve et al., 2013), and ring nematodes feeding on grape roots (Schreiner et al., 2012). Although Esca was not observed on foliage, it is often asymptomatic (Bruez et al., 2014) and may be responsible for vine decline and for apoplectic forms of vine death (Larignon et al., 2009). However, over the studied farm area, a dead fallen arm of vine covered with *Stereum hirsutum* (Willd: Fr.), one of the fungi responsible for wood necrose, was found on the soil surface at the bottom of the BC plot, and symptoms of dead black desease (*Phomopsis viticola (Sacc.) Sacc.* 1915) were observed for some vines. These fungi might be favoured by past and surrounding wood landuse, particularly *Stereum hirsutum* on dead arms of oak trees, as is it very polyphagous (Galet, 1991b).

Further insight into the biological characteristics of the studied soils, that may evidence a long-term and spatially differentiated influence of soil pathogens for instance, or colonization of fine roots by vesicular-arbuscular mycorrhizal fungi (Possingham and Groot Obbink, 1971; Schubert and Cravero, 1985) would be needed. Does vine decline reflect a decrease in mycorrhizal fungi which are known to facilitate nutrient storage and uptake (Schreiner, 2005)? Or else, does it reflect an explosion in soil pathogens?

Besides rootstock and/or disease-induced vine decline, regional-scale process of vine decline in the absence of vine disease symptoms has been reported in Languedoc as soon as 1990s (Legros et al., 1998). Since the 1970s, viticultural techniques have been more and more mechanised, together with the widespread use of chemical pesticides and fertilizers, while fields were restructured and enlarged, often undergoing slope-reshaping by means of heavy machinery (Costantini et al., 2015). Soil degradation caused by intensive viticultural systems was hypothetized as the driving factor for such decline (Lagacherie, 2005; Costantini and Lorenzetti, 2013), particularly in Mediterranean environments, through the concurrent processes of (i) soil loss (Le Bissonnais et al., 2007; Paroissien et al., 2010; Novara et al., 2011), (ii) disturbance of soil layers and outcropping of the underlying unweathered rock or sediment (Costantini et al., 2015), (iii) soil compaction (Lagacherie et al., 2010), (iv) nutrient depletion (Ramos and Martínez-Casasnovas, 2006), (v) soil salinization/sodification under drip-irrigated conditions with moderately saline waters (Aragüés et al., 2014), (vi) pesticide transport in runoff water and pesticide deposition (Louchart et al., 2001, 2004), (vii) copper contamination (El Azzi et al., 2013); (viii) organic matter decline (Costantini and Lorenzetti, 2013; García-Díaz et al., 2016). Of all these processes in the Chauvets farm, processes (i), (iv), and (viii) have been patently playing together. Following the assumptions made by Paroissien et al. (2010) for Mediterranean soils of Languedoc, estimated erosion rates reached 16 $t.ha^{-1}\cdot y^{-1}$ in average (median 10 $t.ha^{-1}\cdot y^{-1}$) and ranged between −20 and 117 $t.ha^{-1}\cdot y^{-1}$, indicating a high spatial variability at the farm scale. Such values were with consistent with previously calculated erosion rates for Mediterranean vineyards using the SUM method (Casalí et al., 2009; Paroissien et al., 2010). For the highest erosion rates (>40 $t.ha^{-1}\cdot y^{-1}$), the first 0.5 m-depth (which is critical for terroir functioning) may be lost in less than 170 y. However, no clear correlation appeared between missing vine frequency and SUM, and, conversely to SUM, the missing vine frequency exhibited a spatial structure only for Grenache. This questions the replicability of mortality spatial structures from farm to district or regional scale, as Lagacherie (2005) observed no spatial structure of vine mortality at a regional scale for Languedoc. Such issue could be further studied using an orthorectified mosaic of ancient photograph time series at the scale of the district; for this a restitution of past practices through interviews to retired winegrowers or collection of other historical records should be needed.

Process (ii) may have worked in the seventies for the planting of plots A and F then in 2001 for the planting of plot F. Processes (iii) and (vi) may not be influential, at least in the 1940s and the 2000s, as no engines circulated because of fertilizers and pesticides shortage or unavailability. For one of the smaller plots (plot G), the high content of easily extractible copper in the upper horizon having the highest root density (154 $\mu g.kg^{-1}$ $CaCl_2$-extractable Cu) was presumably inherited from past orchard: it is questionable whether such high content combined with high clay content (27%) but rather high active lime (12 gKg^{-1}) may have influenced metal bioavailability as observed for Mediterranean soils (de Santiago-Martín et al., 2014) and hence vine decline.

5. Conclusion

This farm-scale approach for viticultural terroir zoning was original in considering both long term series over 70 y and recently acquired remotely-sensed data with very high spatial resolution, jointly with field soil and vine observations and proxy geophysical measurements. Such approach was successful in retracing those zones showing repeated vine mortality over time. It highlighted the tight relationships between vine mortality, soil type, past landuse, and long term soil management, particularly in terms of soil organic carbon.

The increased availability of aerial survey times series, as well as satellite imagery with very high spatial resolution such as Pléiades (70 cm), opens promises for further application of this approach in the years to come, over larger areas, like viticultural districts. While giving prospects for wider applications at different scales, this approach of historical retracing from remote sensing renews questions about the determinism of vine decline, suggesting contribution of soil degradation processes and especially the need for restoring C stocks.

Acknowledgment

This study benefited support for the acquisition of Pléiades images from the French Space Agency (CNES), through the ISIS Programme. It also benefited financial and technical support from the CNES in the framework of the TOSCA PLEIADES-CO program. Special thanks to thank Dalila Hadjar for her help in managing the numerous soil samples.

References

Aragüés, R., Medina, E.T., Clavería, I., Martínez-Cob, A., Faci, J., 2014. Regulated deficit irrigation: soil salinization and soil sodification in a table grape vineyard drip-irrigated with moderately saline waters. Agric. Water Manage. 134, 84–93.

Beuve, M., Moury, B., Spilmont, A.S., Sempé-Ignatovic, L., Hemmer, C., Lemaire, O., 2013. Viral sanitary status of declining grapevine Syrah clones and genetic diversity of Grapevine Rupestris stem pitting associated virus. Eur J. Plant Pathol. 135, 439–452.

Brenot, J., Quiquerez, A., Petit, C., Garcia, J.P., 2008. Erosion rates and sediment budgets in vineyards at 1-m resolution based on stock unearthing (Burgundy, France). Geomorphology 100, 345–355.

Bruez, E., Vallance, J., Gerbore, J., Lecomte, P., Da Costa, J.P., Guerin-Dubrana, L., Rey, P., 2014. Analyses of the temporal dynamics of fungal communities colonizing the healthy wood tissues of Esca leaf-symptomatic and asymptomatic vines. PLoS One 9 (5), 1–15 (e95928).

Casalí, J., Giménez, R., De Santisteban, L., Álvarez-Mozos, J., Mena, J., Del Valle de Lersundi, J., 2009. Determination of long-term erosion rates in vineyards of Navarre (Spain) using botanical benchmarks. Catena 78, 12–19.

Castelan-Estrada, M., Vivin, P., Gaudillère, J.P., 2002. Allometric relationships to estimate seasonal above-ground vegetative and reproductive biomass of Vitis vinifera L. Ann. Bot. 89, 401–408.

Costantini, E.A.C., Bucelli, P., Priori, S., 2012. Quaternary landscape history determines the soil functional characters of terroir. Quat. Int. 265, 63–73.

Costantini, E.A.C., Lorenzetti, M., 2013. Soil degradation processes in the Italian agricultural and forest ecosystems. Italian J. Agron. 8, 233–243.

Costantini, E.A.C., Agnelli, A.E., Fabiani, A., Gagnarli, E., Mocali, S., Priori, S., Simoni, S., Valboa, G., 2015. Short-term recovery of soil physical, chemical, micro and mesobiological functions in a new vineyard under organic farming. Soil 1, 443–457.

Deloire, A., Vaudour, E., Carey, V., Bonnardot, V., Van Leeuwen, C., 2005. Grapevine responses to terroir: a global approach. J. Int. Sci. Vigne Vin 39 (4), 149–162.

Dion, R., 1990. Le Paysage Et La Vigne: Essai De géographie Historique. Payot, Paris.

Dobrowski, S.Z., Ustin, S.L., Wolpert, J.A., 2008. Remote estimation of vine canopy density in vertically shoot-positioned vineyards: determining optimal vegetation indices. Aust. J. Grape Wine R. 8, 117–125.

El Azzi, D., Viers, J., Guiresse, M., Probst, A., Aubert, D., Caparros, J., Charles, F., Guizien, K., Probst, J.L., 2013. Origin and fate of copper in a small Mediterranean vineyard catchment, new insights from combined chemical extraction and δ65Cu isotopic composition. Sci. Total Environ. 463–464, 91–101.

Falipou P., Legros J.P., 2002. Le système STIPA-2000 d'entrée et édition des données pour la base nationale de sols DONESOL II. Etude et Gestion des Sols, 9, 1, 55–70.

Fiorillo, E., Crisci, A., De Filippis, T., Di Gennaro, S.F., Di Blasi, F., Matese, A., Primicerio, J., Vaccari, F.P., Genesio, L., 2012. Airborne high-resolution images for grape classification: changes in correlation between technological and late maturity in a Sangiovese vineyard in Central Italy. Aust. J. Grape Wine Res. 18, 80–90.

Galet, P., 1991a. Précis d'ampélographie pratique. Imprimerie Dehan, Chemin de la Croix de Lavit, Montpellier, France, 256 p.

Galet, P., 1991b. Précis de pathologie viticole. Imprimerie Dehan, Chemin de la Croix de Lavit, Montpellier, France, 264 p.

García-Díaz, A., Bienes Allas, R., Gristina, L., Cerdà, A., Pereira, P., Novara, A., 2016. Carbon input threshold for soil carbon budget optimization in eroding vineyards. Geoderma 271, 144–149.

Hall, A., Louis, J., Lamb, D., 2003. Characterizing and mapping vineyard canopy using high-spatial-resolution aerial multispectral images. Comput. Geosci. 29, 813–822.

Johnson, L.F., 2003. Temporal stability of an NDVI-LAI relationship in a Napa Valley vineyard. Aust. J. Grape Wine R. 9, 96–101.

Löw, F., Michel, U., Dech, S., Conrad, C., 2013. Impact of feature selection on the accuracy and spatial uncertainty of per-field crop classification using support vector machines. ISPRS J. Photogramm. Remote Sens. 85, 102–119.

Lagacherie, P., Collin-Bellier, C., Goma-Fortin, N., 2001. Evaluation et analyse de la variabilité spatiale de la mortalité des ceps dans un vignoble languedocien à partir de photographies aériennes à haute résolution. J. Int. Sci. Vigne Vin 35 (3), 141–148.

Lagacherie, P., Coulouma, G., Ariagno, P., Virat, P., Boizard, H., Richard, G., 2010. Spatial variability of soil compaction over a vineyard region in relation with soils and cultivation operations. Geoderma 134, 207–216.

Lagacherie P. (coord.), 2005. Dégradations physiques des sols de vigne et impacts sur la ressource en eau en milieu méditerranéen viticole. Gessol project report, Montpellier, 101 p. http://www.gessol.fr/content/degradation-physique-des-sols-de-vigne-et-impacts-sur-la-ressource-en-eau-en-milieu-mediterr.

Lanjeri, S., Segarra, D., Melia, J., 2004. Interannual vineyard crop variability in the Castilla-La Mancha region during the period 1991–1996 with Landsat Thematic Mapper images. Int. J. Remote Sens. 25 (12), 2441–2457.

Larignon, P., Fontaine, F., Farine, F., Clément, C., Bertsch, C., 2009. Esca and Black Dead Arm: deux acteurs majeurs des maladies du bois chez la Vigne. C.R. Biologies 332, 765–783.

Le Bissonnais, Y., Blavet, D., De Noni, G., Laurent, J.-Y., Asseline, J., Chenu, C., 2007. Erodibility of Mediterranean vineyard soils: relevant aggregate stability methods and significant soil variables. Eur. J. Soil Sci. 58, 188–195.

Legros, J.P., Argillier, J.P., Callot, G., Carbonneau, A., Champagnol, F., 1998. Les sols viticoles du Languedoc: un état préoccupant. Progrès Agricole et Viticole 13–14, 296–298.

Louchart, X., Voltz, M., Andrieux, P., Moussa, R., 2001. Herbicides transport at field and watershed scales in a Mediterranean vineyard area. J. Environ. Qual. 30, 982–991.

Louchart, X., Voltz, M., Coulouma, G., Andrieux, P., 2004. Oryzalin fate and transport in runoff water in Mediterranean vineyards. Chemosphere 57, 921–930.

Mehra, O.P., Jackson, M.L., 1960. Iron oxide removal from soils and clays by a dithionite-citrate system buffered with sodium bicarbonate. In Clays and Clay Minerals. In: Proceedings of the 7th Conference, Nat1 Acad. Sci-Nat1 Res. Council Publ., Washington DC, pp. 317–327.

Novara, A., Gristina, L., Saladino, S.S., Santoro, A., Cerdà, A., 2011. Soil erosion assessment on tillage and alternative soil managements in a Sicilian vineyard. Soil Till. Res. 117, 140–147.

Pal, M., Mather, P.M., 2004. Assessment of the effectiveness of support vector machines for hyperspectral data. Future Gener. Comput. Syst. 20, 1215–1225.

Palomares-Rius, J.E., Gutiérrez-Gutiérrez, C., Cantalapiedra-Navarrete, C., Castillo, P., 2012. Prevalence and diversity of Grapevine fanleaf virus in southern Spain. Plant Pathol. 61, 1032–1042.

Paroissien, J.B., Lagacherie, P., Le Bissonnais, Y., 2010. A regional scale study of multi-decennial erosion of vineyard fields using vine-stock unearthing–burying measurements. Catena 82, 159–168.

Pebesma, E.J., 2004. Multivariable geostatistics in S: the gstat package. Comput. Geosci. 30 (7), 683–691.

Pebesma, E.J., 2014. Gstat user's manual, 108 p. http://www.gstat.org/.

Pedroso, M., Taylor, J., Tisseyre, B., Charnomordic, B., Guillaume, S., 2010. A segmentation algorithm for the delineation of agricultural management zones. Comput. Electron. Agr. 70, 199–208.

Pellegrino, A., Lebon, E., Voltz, M., Wery, J., 2004. Relationships between plant and soil water status in vine (Vitis vinifera L.). Plant and Soil 266, 129–142.

Possingham, J.V., Groot Obbink, J., 1971. Endotrophic myccorhiza and the nutrition of grape vines. Vitis 10, 120–130.

Priori, S., Martini, E., Andrenelli, M.C., Magini, S., Agnelli, A.E., Bucelli, P., Biagi, M., Pellegrini, S., Costantini, E.A.C., 2013. Improving wine quality through harvest zoning and combined use of remote and proximal sensing. Soil Sci. Soc. Am. J. 77, 1338–1348.

Quiquerez, A., Chevigny, E., Allemand, P., Curmi, P., Petit, C., Grandjean, P., 2014. Assessing the impact of soil surface characteristics on vineyard erosion from very high spatial resolution aerial images (Côte de Beaune, Burgundy, France). Catena 116, 163–172.

Ramos, M.C., Martínez-Casasnovas, J.A., 2006. Nutrient losses by runoff in vineyards of the Mediterranean Alt Penedès region (NE Spain). Agriculture. Ecosyst. Environ. 113, 356–363.

Richter, R., Schläpfer, D., 2014. ATCOR-2/3 user guide, version 8.3.1, Zurich, Switzerland, 238 p.

Rossi, R., Pollice, A., Diago, M.P., Oliveira, M., Millan, B., Bitella, G., Amato, M., Tardaguila, J., 2003. Using an automatic resistivity profiler soil sensor on-the-go in precision viticulture. Sensors 13, 1121–1136.

Schabenberger, O., Gotway, C.A., 2005. Statistical Methods for Spatial Data Analysis. Chapman&Hall/CRC, Boca Raton, USA.

Schreiner, P., 2005. Spatial and temporal variation of roots, arbuscular mycorrhizalfungi, and plant and soil nutrients in a mature Pinot Noir (Vitis vinifera L.) vineyardin Oregon, USA. Plant and Soil 276, 219–234.

Schreiner, R.P., Pinkerton, J.N., Zasada, I.A., 2012. Delayed response to ring nematode (Mesocriconema xenoplax) feeding on grape roots linked to carbohydrate reserves and nematode feeding pressure. Soil Biol. Biochem. 45, 89–97.

Schubert, A., Cravero, M.C., 1985. Occurrence and infectivity of vesicular-arbuscular mycorrhizal fungi in north-western Italy vineyards. Vitis 24, 129–138.

Seguin, G., 1986. « Terroirs » and pedology of wine growing. Experientia 42 (8), 861–873.

Tardaguila, J., Baluja, J., Arpon, L., Balda, P., Oliveira, M., 2011. Variations of soil properties affect the vegetative growth and yield components of "Tempranillo" grapevines. Precis. Agric. 12, 762–773, http://dx.doi.org/10.1007/s11119-011-9219-4.

Tomasi, D., Gaiotti, F., Jones, G.V., 2013. The Power of the Terroir: the Case Study of Prosecco Wine. Springer, Basel.

Tomasi, D., Battista, F., Gaiotti, F., Mosetti, D., Bragato, G., 2015. Soil influence on root distribution and implications for berry and wine quality of the Tocai Friulano variety. Am. J. Enol. Vitic. 66 (3), 363–372.

Unwin, T., 1991. Vine and the Wine: an Historical Geography of Viticulture and the Wine Trade. Routledge, London.

Van Leeuwen, C., Friant, P., Choné, X., Tregoat, O., Koundouras, S., Dubourdieu, D., 2004. The influence of climate, soil and cultivar on terroir. Am. J. Enol. Vitic. 55, 207–217.

Vaudour, E., Girard, M.C., Brémond, L.M., Lurton, L., 1998. Caractérisation spatiale et constitution des raisins en AOC Côtes-du-Rhône méridionales (Bassin de Nyons-Valréas). J. Int. Sci. Vigne Vin 32 (4), 169–182.

Vaudour, E., Carey, V.A., Gilliot, J.M., 2010. Digital zoning of South African viticultural terroirs using bootstrapped decision trees on morphometric data and multitemporal SPOT images. Remote Sens. Environ. 114, 2940–2950.

Vaudour, E., Carey, V.A., Gilliot, J.M., 2014a. Multidate remote sensing approaches for digital zoning of terroirs at regional scales: case studies and perspectives. Geophysical Research Abstracts, vol. 16, EGU2014-11533, EGU General Assembly 2014, Vienna (Austria).

Vaudour, E., Gilliot, J.M., Bel, L., Bréchet, L., Hadjar, D., Hamiache, J., Lemonnier, Y., 2014b. Uncertainty of soil reflectance retrieval from SPOT and RapidEye multispectral satellite images using a per-pixel bootstrapped empirical line atmospheric correction over an agricultural region. Int. J. Appl. Earth Obs. Geoinf. 26, 217–234.

Vaudour, E., Costantini, E., Jones, G., Mocali, S., 2015a. An overview of the recent approaches for terroir functional modelling, footprinting and zoning. Soil 1, 287–312, http://dx.doi.org/10.5194/soil-1-287-2015.

Vaudour, E., Noirot-Cosson, P.E., Membrive, O., 2015b. Early-season mapping of crops and cultural operations using very high spatial resolution Pléiades images. Int. J. Appl. Earth Observ. Geoinf. 42, 128–141.

Vaudour, E., 2002. The quality of grapes and wine in relation to geography: notions of terroir at various scales. J. Wine Res. 13 (2), 117–141.

Vaudour, E., 2003. Les Terroirs Viticoles. Dunod, Paris.

World Reference Base (WRB), 2014. World Reference Base for Soil Resources. A Framework for International Classification, Correlation and Communication. Food and Agriculture Organization of the United Nations, Rome, pp. 128.

de Santiago-Martín, A., Valverde-Asenjo, I., Quintana, J.R., Vásquez, A., Lafuente, A.L., González-Huecas, C., 2014. Carbonate, organic and clay fractions determine metal bioavailability in periurban calcareous agricultural soils in the Mediterranean area. Geoderma 221–222, 103–112.